

# EFFECT OF MICROSTRUCTURE AND SPATIAL INHOMOGENEITIES OF A DISPERSE MEDIUM ON MULTIPLE LIGHT SCATTERING IN THE SMALL-ANGLE APPROXIMATION

V.V. Veretennikov

*Institute of Atmospheric Optics,  
Siberian Branch of the Russian Academy of Sciences, Tomsk*

*Received April 23, 1993*

*The trends in the behavior of the optical transfer function and point spread function of a scattering layer caused by changing its position and optical and geometric thicknesses are numerically studied in the small-angle approximation. A specific feature of the solution method is that the Fourier transform of a small-angle scattering phase function is represented in the form of an autocorrelation function of particle shadow. This allows the relation of optical properties of the medium to its disperse composition to be determined.*

## 1. INTRODUCTION

Much attention is currently given to the solution of inverse problems for optics of disperse media in the case of multiple light scattering in connection with the problem of sounding of dense aerosol formations. The efficiency of the solution of such problems depends strongly on the structure and bulk of measurement information as well as on the experimental configuration and viewing geometry. One of the promising directions in this area is based on the small-angle approximation of radiative transfer theory. This approximation was used in Ref. 1 to construct the algorithms for reconstructing a disperse composition of the scattering media from the data on the angular distribution of a multiply scattered plane wave.

The use of narrow laser beams in laser radar techniques initiated the study of the irradiance distribution over the beam cross section as a function of the optical thickness and the microstructural parameters of a scattering medium. The point spread function (PSF) plays an important role in the determination of the irradiance produced by a light field.<sup>2,3</sup>

The goal of the present paper is to study the basic trends in the behavior of the PSF and its Fourier transform, the optical transfer function (OTF), in the small-angle approximation as functions of the disperse structure of the medium characterized by the particle size distribution function and particle concentration field which is uniquely related to the spatial distribution of the extinction coefficient. The problems under discussion have not yet been studied adequately in the papers concerned with the analysis of the PSF in the scattering media since these papers deal primarily with the solution of the radiative transfer equation (RTE) in which the explicit dependences on the disperse characteristics of a medium are lacking. This is especially true in regard to the representation of the scattering phase function which in the small-angle approximation is usually described by the rapidly damped exponential function  $a^2 \exp(-a\theta)$  (Ref. 4), the Gaussian function  $a \exp(-a\theta^2)$  (Ref. 5), and the function  $a\theta^{-1} \exp(-a\theta)$  (Ref. 2), where  $\theta$  is the scattering angle.

The results obtained in this paper may be useful in the design of the experiments and estimation of the information content of the inverse problems in reconstructing macro- and microstructural parameters of the disperse media in the case of multiple light scattering.

The problem under study may also be of interest in the optical signal transfer through dense scattering media and the

estimation of the effect of structural properties of the medium on the parameters of transmitted signal (optical communication and transfer of images through turbid media).

## 2. INITIAL RELATIONS

To solve the formulated problem, we start from representation of the Fourier transform of the small-angle scattering phase function in the form of the autocorrelation function of a mean particle shadow<sup>6</sup>

$$\varphi(\rho) = \int_{r/2}^R G(\rho/2r) f(r) dr, \quad 0 \leq \rho \leq 2R, \quad (1)$$

where  $f(r) = s(r)/S$ ,  $s(r) = \pi r^2 n(r)$ , and  $n(r)$  is the distribution of number density of particles over size;

$S = \int_0^R s(r) dr$  is the total geometric cross section of particles in unit volume of the scattering medium;  $G(\rho/2r)$  is the autocorrelation coefficient of the shadow from the spherical particle of radius  $r$ ,

$$G(t) = \begin{cases} 2\pi^{-1} [\arccos(t) - t(1-t^2)^{1/2}], & t \leq 1, \\ 0, & t > 1. \end{cases} \quad (2)$$

Expression (1) describes the Fraunhofer diffraction when an ensemble of particles is replaced by a system of independent opaque plane screens, which is allowable for  $\kappa r |m-1| \gg 1$ , where  $m$  is the complex refractive index of particles,  $\kappa = 2\pi/\lambda$ , and  $\lambda$  is the wavelength.

Let the radiation be incident on a medium in the positive direction of the  $OZ$  axis and the volume coefficients of extinction  $\varepsilon(z)$  and scattering  $\sigma(z)$  be functions of the coordinate  $z$ . Then with allowance for the fact that relations  $\varepsilon = 2S$  and  $\sigma = S$  are valid in the case of scattering by large particles ( $r \gg \lambda$ ), the OTF of the medium  $F(v)$  in the small-angle approximation is expressed immediately in terms of the geometric parameters of the particle in the form<sup>7</sup>

$$F(v) = \exp \{ -\tau(z) + g(v) \}, \quad (3)$$

where

$$\tau(z) = \int_0^z \varepsilon(t) dt, \tag{4}$$

$$g(v) = \int_0^z S(z-t)\varphi(vt/\kappa) dt, \tag{5}$$

$v$  is the spatial frequency, and  $\tau$  is the optical depth of the medium in the layer  $[0, z]$ . The PSF of the medium  $E(r)$  is the Hankel transform of the function  $F(v)$  given by Eq. (3):

$$E(r) = \frac{1}{2\pi} \int_0^\infty v J_0(vr) F(v) dv. \tag{6}$$

In addition to the PSF  $E(r)$  describing the spatial distribution of the irradiance over the plane  $z = \text{const}$ , we also consider the radiant flux  $P(r)$  which flows through a circular area centered on the  $OZ$  axis and oriented perpendicular to the direction of incident radiation propagation

$$P(r) = r \int_0^\infty J_1(rv) F(v) dv. \tag{7}$$

The PSF  $E(r)$  is expressed in terms of the derivative of  $P(r)$

$$E(r) = \frac{1}{2\pi r} \frac{dP(r)}{dr}. \tag{8}$$

The optical characteristics of the medium  $F(v)$ ,  $E(r)$ , and  $P(r)$  can be represented as a sum of the transmitted attenuated (denoted by the subscript 0) and scattered (sc) radiations

$$F(v) = F_0 + F_{sc}(v), \tag{9}$$

$$E(r) = E_0(r) + E_{sc}(r), \tag{10}$$

$$P(r) = P_0(r) + P_{sc}(r), \tag{11}$$

where

$$F_0 = P_0 = e^{-\tau}, \tag{12}$$

$$F_{sc}(v) = \exp\{-\tau + g(v)\} - \exp(-\tau). \tag{13}$$

For the transmitted radiation  $E_0(r) = \sigma(r)e^{-\tau}$ , the functions  $E_{sc}(r)$  and  $P_{sc}(r)$  are found from expressions analogous to Eqs. (6) and (7) with  $F(v)$  replaced by  $F_{sc}(v)$ . It should be noted that everywhere, with the exception of the point  $r = 0$ ,  $E_{sc}(r) = E(r)$ . As  $r \rightarrow \infty$ , formula (11) transforms into the relation for net fluxes flowing through the plane  $z = \text{const}$

$$B(\tau) = B_0 + B_{sc} = \exp(-\tau/2),$$

$$B_0(\tau) = e^{-\tau}, \quad B_{sc}(\tau) = \exp(-\tau/2) - \exp(-\tau). \tag{14}$$

### 3. QUALITATIVE ANALYSIS OF THE OPTICAL CHARACTERISTICS

When radiation propagates through the monodisperse media, the OTF and PSF of two media with different particle radii  $R_1$  and  $R_2$  satisfy the relations of similarity

$$F_2(v) = F_1(v/q), \quad E_2(r) = q^2 E_1(qr), \tag{15}$$

where  $q = R_2/R_1$ . Relations (15) can be generalized to polydisperse ensembles of particles which have analogous functions of distribution  $f(\eta)$  over the relative radius  $\eta = r/R_e$  with  $R$  replaced by the effective radius  $R_e$  for which we have assumed, e.g., the rms radius, etc.

It follows from the property of monotony of the function  $F(v)$  and relation (15) that  $F_2(v) > F_1(v)$  when  $R_{e2} > R_{e1}$ , i.e., with an increase of the effective radius of scatterers, broadening of the OTF of the medium occurs. In the near-axis region where the function  $E(r)$  decreases monotonically, for  $R_{e2} > R_{e1}$ , the inequality is fulfilled

$$\frac{E_{sc,2}(r)}{E_{sc,2}(0)} < \frac{E_{sc,1}(r)}{E_{sc,1}(0)}, \tag{16}$$

which indicates that the transverse scale of a light beam decreases with increase of the effective radius of scatterers.

Starting from the properties of the function  $G(t)$  given by Eq. (2) and nonnegative character of the extinction coefficient  $\varepsilon(z)$ , it can be shown for the function  $g(v)$  given by Eq. (5) that

$$0 \leq g(v) \leq \tau/2, \quad g'(v) \leq 0, \quad g''(v) \geq 0, \tag{17}$$

from which follow the analogous properties of the OTF  $F(v)$  of the medium given by Eq. (3):

$$0 < F(v) \leq F(0), \quad F'(v) \leq 0, \quad F''(v) \geq 0, \tag{18}$$

where  $F(0) = B(\tau)$  defines the net radiative flux flowing through the plane  $z = \text{const}$ . If we additionally assume that the scattering layer is at the distance  $H$  from the observation point, then  $g(v) = 0$  and hence  $F_{sc}(v) = 0$  for  $v > v_{\text{max}} = 2\kappa R/H$ . Thus the OTF of the medium  $F(v)$  in the small-angle approximation is a bounded monotonically decreasing function being convex downwards.

The width of the function  $F_{sc}(v)$  can be judged from the position of the point of intersection of the abscissa and a tangent to the curve  $F_{sc}(v)$  passing through zero, which is defined by the relation

$$v^* = \mu/|g'(0)|. \tag{19}$$

The quantity  $v^*$  also determines the frequency at which the OTF  $F_{sc}(v)$  is by a factor of  $e$  smaller than its maximum value for exponential approximation of  $F_{sc}(v)$ :

$$F_{sc}(v) = F_{sc}(0) \exp(-v/v^*). \tag{20}$$

The coefficient  $\mu$  specifies the relative contribution of scattered radiation to the net flux and monotonically increases from 0 to 1 as a function of the optical depth  $\tau$

$$\mu(\tau) = B_{sc}/B = 1 - \exp(-\tau/2), \tag{21}$$

where  $B$  and  $B_{sc}$  are found from Eq. (14). Following Ref. 7, the quantity  $g'(0)$  is

$$|g'(0)| = \frac{L\tau}{\pi \kappa R_e}, \tag{22}$$

where  $L$  is the distance from the observation point to the center of gravity of the scattering layer ( $L = z/2$  when  $\varepsilon = \text{const}$ ) and  $R_e$  is the effective size of scatterers found from the formula

$$R_e = \left[ \int_0^R f(r) r^{-1} dr \right]^{-1} \quad (23)$$

Using Eqs. (19)–(23), we finally obtain the estimate of the frequency  $\nu^*$

$$\nu^* = \nu_1 \omega(\tau), \quad (24)$$

where

$$\nu_1 = \frac{\pi \kappa R_e}{2L}. \quad (25)$$

The quantity  $\nu_1$  specifies the OTF width of the medium  $F_{sc}(\nu)$  in the single-scattering approximation and the factor

$$\omega(\tau) = \frac{1 - \exp(-\tau/2)}{\tau/2} \quad (26)$$

is the monotonically decreasing function within the region of its variation  $0 > \omega(\tau) \leq 1$ . In this case  $\omega(\tau) \rightarrow 1$  and  $\nu^* \rightarrow \nu_1$  as  $\tau \rightarrow 0$ . The function  $\omega(\tau)$  describes the effect of multiple scattering on the width of the frequency spectrum  $F_{sc}(\nu)$ . Thus, as seen from Eqs. (24)–(26), the OTF width decreases monotonically with increase of optical density of the medium. The frequency  $\nu^*$  is proportional to the effective radius of particles  $R_e$  given by Eq. (23) and decreases with increase of the distance to the layer  $L$ .

As an example, Table I gives the values of  $\nu^*$  obtained from formula (19) by way of numerical estimate of the derivative of the function  $g(\nu)$  given by Eq. (5) for zero value of the argument at the wavelength  $\lambda = 0.55 \mu\text{m}$  for different positions of the scattering layer which was modelled by a Gaussian curve with the mean distance  $z_m$  and variance  $\sigma^2$  for the following fixed values of the parameters of the medium:  $R_e = 10 \mu\text{m}$ ,  $\tau = 1$ , and  $\sigma = 0.5 \text{ km}$ .

TABLE I.

$z_m, \text{ km}$	$\nu^*, \text{ km}^{-1}$	$r^*, \text{ km}$	
		$\varepsilon = 0.1$	$\varepsilon = 0.2$
2	17.6	0.565	0.278
5	28.36	0.351	0.173
8	70.96	0.140	0.069

The spatial scale of the PSF  $E(r)$  can be characterized by the radius of the area  $r^*$  on which the given fraction of the scattered light flux  $(1 - \varepsilon)$  is incident

$$\frac{P_{sc}(r^*)}{B_{sc}} = \frac{2\pi}{F_{sc}(0)} \int_0^{r^*} F_{sc}(r) r dr = (1 - \varepsilon). \quad (27)$$

With the exponential approximation of the OTF  $F_{sc}(\nu)$  given by Eq. (20), the solution  $r^*$  of Eq. (27) has the form

$$r^* = 1/\nu^*(1/\varepsilon^2 - 1)^{1/2}, \quad (28)$$

where  $\nu^*$  is found from Eq. (19). For aforementioned example the estimates  $r^*$  of the width of the PSF  $E(r)$  by formula (28) with  $\varepsilon = 0.1$  and  $0.2$  are given in Table I.

#### 4. RESULTS OF NUMERICAL MODELING

In the numerical experiments the scattering layer along the path of the length  $z = 10 \text{ km}$  was modeled by normal distribution with the mean distance  $2 \leq z_m \leq 8 \text{ km}$ , variance

$\sigma^2$  ( $0.1 \leq \sigma \leq 1$ ), and optical depth  $1 \leq \tau \leq 8$ . The dependences considered below were obtained at the wavelength  $\lambda = 0.55 \mu\text{m}$  for the effective radius of particles  $R_e = 10 \mu\text{m}$ . Transformation to analogous dependences at other wavelengths for other effective radii of particles is accomplished following the similarity relations given by formulas (15).

Depicted in Fig. 1a are the dependences of the PSF  $E(r)$  obtained for different positions of the scattering layer, determined by different values of  $z_m$ , and fixed values of the parameters  $\tau$  and  $\sigma$ . As seen from Fig. 1a, the behavior of the function  $E(r)$  is strongly affected by the spatial structure of the extinction coefficient profile  $\varepsilon(z)$ . As follows from Fig. 1b, in which the normalized dependences  $E_{sc}(r)/E_{sc}(0)$  are shown, the spatial redistribution of the light flux over extended area takes place as the scattering layer moves away from the observation point (i.e., with decrease of  $z_m$ ). Since in this case the net flux flowing through the cross section  $B(\tau)$  given by Eq. (14) remains unchanged, the beam broadening causes the decrease of irradiance in the near-axis region (see Fig. 1a).

The results of calculation of the normalized fluxes of scattered radiation  $P_{sc}(r)/B_{sc}$  depicted in Fig. 2 correspond to a family of dependences of the PSF  $E(r)$  shown in Figs. 1a and b. As seen from Fig. 2 and Table I, the dimensions of the beam cross section, within which a specific portion of light energy propagates, are in satisfactory agreement with the estimates of  $r^*$  by formulas (27) and (28).

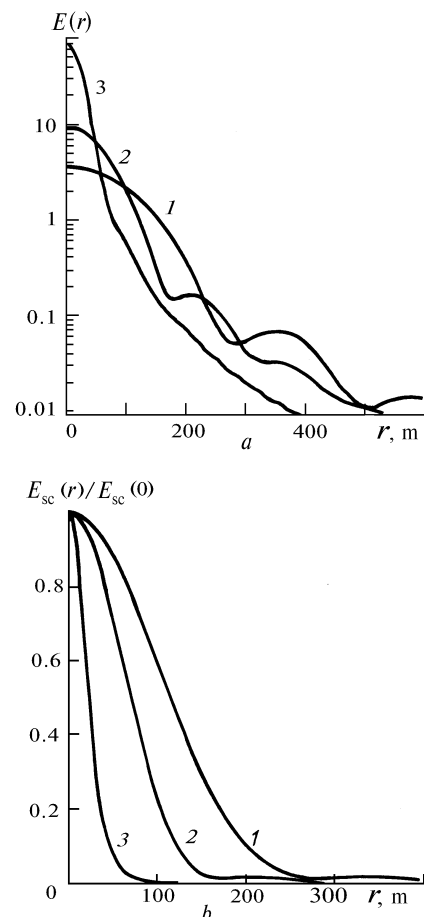


FIG. 1. Irradiance distribution  $E(r)$  (a) and the ratio  $E_{sc}(r)/E_{sc}(0)$  (b) in the plane  $z = 10 \text{ km}$  for different positions of the scattering layer and constant values of its geometric thickness ( $\sigma = 0.5 \text{ km}$ ) and optical depth ( $\tau = 1$ ).  $z_m = 2$  (1),  $5$  (2), and  $8 \text{ km}$  (3).

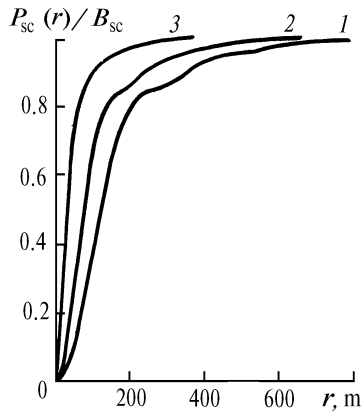


FIG. 2. The ratio of the flux of scattered radiation  $P_{sc}(r)$  flowing through the circular area of radius  $r$  to the net scattered flux  $B_{sc}$  for different positions of the layer.  $z_m = 2$  (1), 5 (2), and 8 km (3). The remaining parameters of the layer are the same as in Fig. 1.

Figure 3 illustrates the effect of the scattering layer thickness, for fixed position of its center, on the behavior of the PSF  $E(r)$ . Curves 1–3 in Fig. 3 correspond to the values of the parameters  $\sigma = 0.1, 0.5,$  and  $1.0$  km at  $z_m = 5$  km. The functions  $E(r)$  depicted in Fig. 3 have identical effective widths, and distinctive features are manifested in the near-axis region (see Fig. 3b) and on the periphery of the beam. The intensification of irradiance at the beam center with increase of the layer thickness is accounted for by the increase of the cutoff frequency  $\nu_{max}$  at which the OTF vanishes as well as by the properties of monotony and convexity of the function  $F_{sc}(\nu)$ . The value of the frequency  $\nu_{max}$  is inversely proportional to the distance  $H$  from the observation point to the nearest boundary of the layer which is displaced towards the observation point with increase of the layer thickness.

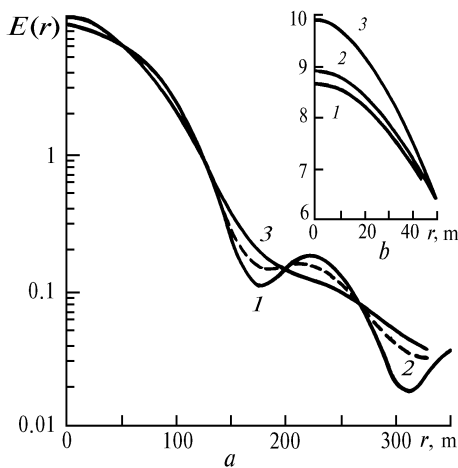


FIG. 3. Irradiance distribution at different geometric thicknesses of the layer for fixed position of its center ( $z_m = 5$  km and  $\tau = 1$ ).  $\sigma = 0.1$  (1), 0.5 (2), and 1 km (3).

The dependence of the PSF  $E(r)$  on the beam periphery (see Fig. 3b) exhibits periodic oscillations which are smoothed out with increase of geometric extension of the layer. These oscillations are engendered by the effect of the scattering phase function, the essence of which is as

follows. Using the expansion of the exponent  $\exp g(\nu)$  in a series and considering a linear term as well as taking into account the relation between the shadow correlation function  $\phi(\rho)$  and the small-angle scattering phase function  $x(\theta)$  (see Ref. 1), we obtain the expressions for the OTF  $F_1(\nu) = e^{-\tau}g(\nu)$  and the PSF of the medium in the single scattering approximation

$$E_1(r) = \frac{1}{4\pi} e^{-\tau} \int_0^z \sigma(z-t) x(r/t) t^{-2} dt. \tag{29}$$

Formula (29) has a simple physical sense. The irradiance at the point  $r$  is formed by contributions of the volume elements, located along the  $OZ$  axis at different distances  $t$  from the observation plane, which scatter the radiation within the directions  $\theta = r/t$ . With decrease of the geometric thickness of the scattering layer, when the optical depth  $\tau$  remains unchanged, we obtain in the limit

$$E_1(r) = \frac{\tau e^{-\tau}}{8\pi L^2 x(r/L)}, \tag{30}$$

where  $L$  is the distance from an infinitely thin layer to the observation point. As known, in the particular case of the medium consisting of particles of the same radius  $R$ ,  $x(\theta) = 4 J_1^2(\kappa R \theta)/\theta^2$ , where  $J_1(y)$  is the first order Bessel function. Zeros  $y_i$  of the Bessel function  $J_1(y)$  correspond to the positions of the minima

$$r_i(r) = \frac{L}{\kappa R_e} y_i \tag{31}$$

in curves 1 and 2 in Fig. 3a. An increase in the geometric thickness of the layer causes the minima of the scattering phase function  $x(r/t)$  in integrand (29) with different  $t$  to be shifted relative to each other. This results in smoothing out the observed oscillations in the irradiance distribution  $E(r)$ . The oscillations of the function  $E_1(r)$  are also smoothed out due to averaging of the scattering phase function  $x(\theta)$  over the particle size spectrum. Of particular attention in Fig. 3a are the points  $r_j \approx 196, 272,$  and  $342$  m in the curves  $E(r)$ , located between the corresponding extrema of the Bessel function  $J_1(y)$ , in the vicinity of which the irradiance remains practically unchanged under variations in the thickness of the scattering layer. These regions, naturally, contain no information about the geometric thickness of the layer.

In conclusion we consider the effect of the optical depth  $\tau$  on the behavior of the PSF of the medium. The net flux of the scattered radiation flowing through the plane  $z = \text{const}$  is described by the function  $B_{sc}(\tau)$  given by Eq. (14) which reaches maximum of 0.25 at  $\tau = 2 \ln 2 \approx 1.39$ , while the component of the flux formed due to the  $k$ th order scattering attains its maximum at  $\tau = \kappa$ . In particular, the flux of the singly scattered radiation is maximum at  $\tau = 1$ . The relative contribution of the flux of the singly scattered radiation is determined from the expression

$$\frac{B_1(\tau)}{B_{sc}(\tau)} = \frac{\tau/2}{\exp(\tau/2) - 1} = \delta_1(\tau). \tag{32}$$

The function  $\delta_1(\tau)$  equals 1 at  $\tau = 0$  and decreases monotonically with  $\tau$  increase down to  $\delta_1(\tau) = 0.5$  at  $\tau \approx 2.48$ . Hence, the contribution of the singly scattered

radiation to the net scattered flux, even decreasing for  $\tau > 1$ , remains dominant up to the optical thickness  $\tau \approx 2.48$ , and only at larger values of  $\tau$  the contribution of multiple scattering exceeds that caused by single scattering.

The relative contribution of scattered radiation of different multiplicity also changes in the beam cross section in going from its center to periphery. Let us consider the effect of density of the medium on spatial distribution of irradiance over the plane  $z = \text{const}$ . Depicted in Fig. 4 are normalized dependences of the PSF  $E_{sc}(r)/E_{sc}(0)$  for the Gaussian profile of the extinction coefficient with the parameters  $z_m = 5$  and  $\sigma = 0.5$  km for three values of the optical depths  $\tau = 1, 5$ , and  $8$  (curves 1–3, respectively). The flux of the scattered energy is redistributed over an extended area with simultaneous decrease of the net scattered flux (for  $\tau > 1.39$  in accordance with Eq. (14)) due to the increase of contribution from multiple scattering with  $\tau$ . In this case the relative contribution of multiply scattered radiation increases in going from the center of the beam to its edge. At small optical depths, when the contribution of singly scattered light is significant ( $\delta_1(1) \approx 0.77$ ), the oscillations engendered by the aforementioned effect of scattering phase function are observed in the behavior of the function  $E_{sc}(r)$  (curve 1, Fig. 4) on the periphery of the beam. These oscillations are smoothed out when the multiply scattered radiation component is added (curves 2 and 3 in Fig. 4).

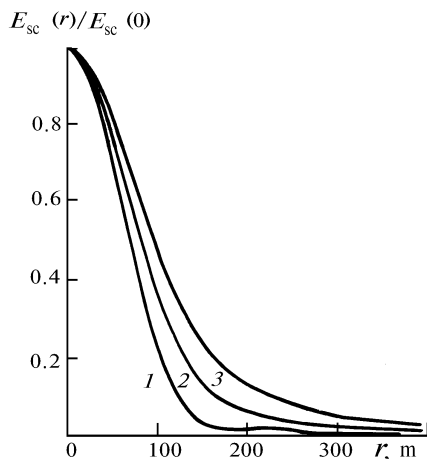


FIG. 4. Normalized distribution of irradiance  $E_{sc}(r)/E_{sc}(0)$  over the beam cross section for the Gaussian profile of the extinction coefficient with the parameters  $z_m = 5$  km and  $\sigma = 0.5$  km as a function of the optical depth of the layer  $\tau = 1$  (1), 5 (2), and 8 (3).

Figure 5 shows the plots of normalized fluxes  $P_{sc}(r)/B_{sc}$  at different optical depths of the medium. Curves 1–4 are for  $\tau = 1, 2, 5$ , and  $8$ . The values of the remaining parameters of the medium are the same as in Fig. 4. In the curves of Fig. 5 it is possible to separate out a central region with rapid increase of the value of the scattered flux  $P_{sc}(r)$  transforming into the saturation region with smooth tendency of  $P_{sc}(r)$  to  $B_{sc}$ . The estimates  $r^*$  of the width of the PSF  $E_{sc}(r)$  at different optical depths  $\tau$  listed in Table II were obtained from the data of Fig. 5 according to Eq. (27) for  $\epsilon = 0.1$ . Table II also gives the values of the function  $c/\omega(\tau)$  which approximates the dependence of  $r^*$  on  $\tau$ , where  $c = \text{const}$  and  $\omega(\tau)$  is

determined by formula (26). The rms error of approximation is about 4%.

TABLE II.

$\tau$	1	2	5	8
$r^*, \text{ km}$	0.246	0.315	0.492	0.738
$c/\omega(\tau)$	0.231	0.291	0.499	0.747

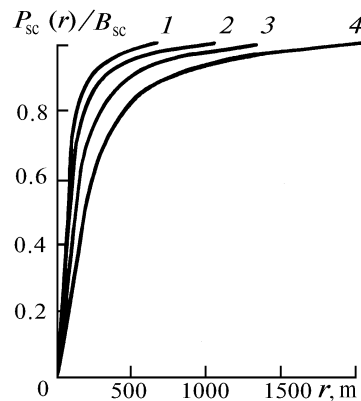


FIG. 5. The ratio of the flux of scattered radiation  $P_{sc}(r)$  flowing through the circular area of radius  $r$  to the net scattered flux  $B_{sc}(r)$  for different optical depths of the layer  $\tau = 1$  (1), 2 (2), 5 (3), and 8 (4). The remaining parameters of the layer are the same as in Fig. 4.

Figure 6 depicts a family of dependences  $h(\tau, r) = P_{sc}(r)/P_0$  which describes the behavior of the ratio of the scattered radiation flux  $P_{sc}(r)$  to the unscattered flux  $P_0$  at  $\tau = 1, 2, 3$ , and  $5$  (curves 1–4, respectively). It is clear that as  $r \rightarrow \infty$ , the function  $h(\tau, r)$  tends to the limit  $h(\tau) = B_{sc}/B_0 = e^{\tau/2} - 1$ . The function  $h(\tau)$  is monotonically increasing and unbounded, i.e., with increase of the optical depth  $\tau$  the contribution of the scattered radiation to the net flux increases while the contribution of the flux of directly transmitted radiation decreases monotonically, and at the instant both fluxes become equal ( $h(\tau) = 1$  at  $\tau \approx 1.39$ ), the net flux of the scattered radiation reaches its maximum ( $B_{sc} = 0.25$ ).

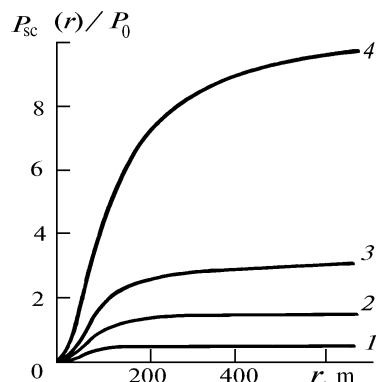


FIG. 6. The ratio of the scattered radiation flux  $P_{sc}(r)$  flowing through the circular area of radius  $r$  to the unscattered flux  $P_0$  for different optical depths of the layer  $\tau = 1$  (1), 2 (2), 3 (3), and 5 (4). The remaining parameters of the layer are the same as in Figs. 4 and 5.

The behavior of the ratio of the scattered and unscattered radiation fluxes  $h(\tau, r)$  flowing through a bounded area of radius  $r$  is analogous – it increases monotonically with  $\tau$ . Figure 6 allows one to estimate the radius  $r_1$  of the region in which the fluxes of scattered  $P_{sc}(r)$  and unscattered  $P_0$  radiations become equal. The value of  $r_1$  is found from the solution of the equation  $h(\tau, r) = 1$ . When  $\tau = 1$ , the solution of this equation does not exist (curve 1 of Fig. 1 does not intersect the straight line  $h = 1$ ). When  $\tau = 2\ln 2$ , the fluxes become equal only at infinity as  $r \rightarrow \infty$ . As the optical depth increases further, the parameter under study decreases monotonically down to  $r_1 = 105$  m at  $\tau = 2$  and  $r_1 = 25$  m at  $\tau = 8$ .

Comparing the results shown in Figs. 1 and 4 we see that the effects engendered by multiple scattering, which intensify with increase of the optical depth  $\tau$ , may alter the behavior of the irradiance  $E(r)$  in the plane  $z = \text{const}$  (resulting in beam broadening and oscillation smoothing) and are qualitatively similar to those engendered by the peculiarities of the spatial structure of the extinction coefficient (position of the layer and its thickness).

### 5. CONCLUSION

In conclusion three principal factors can be distinguished which affect the behavior of the OTF and PSF of the scattering medium. First, it is the microstructure of the medium which determines the form of the scattering phase function. Second, it is a set of the parameters which describe the spatial distribution of scatterer concentration, i.e., the structure of the medium on a macroscale. And third, it is the optical depth of the medium which is the governing factor in the formation of the multiply scattered radiation background.

In accordance with the foregoing factors, the basic regularities in the transformation of the PSF and OTF have been found and their effective scales have been estimated. The results of numerical modeling serve as the basis for estimating the effect of the parameters of disperse media on the energy characteristics of optical signals in problems of sounding, communication, vision, etc.

It has been shown that the factors of different origin such as, e.g., the particle radius and position of the scattering layer or distance to the layer and its optical depth have analogous effects on the structure of the parameters under study. Therefore, it should be taken into account that cooperative manifestation of these factors in the optical experiments makes their interpretation difficult.

### REFERENCES

1. N.I. Vagin and V.V. Veretennikov, *Izv. Akad. Nauk SSSR, Fiz. Atmos. Okeana* **25**, No. 7, 723–731 (1989).
2. D.M. Bravo–Zhivotovskii, L.S. Dolin, A.G. Luchinin, and V.A. Savel'ev, *Izv. Akad. Nauk SSSR, Fiz. Atmos. Okeana* **5**, No. 2, 160–167 (1969).
3. E.P. Zege, A.P. Ivanov, and I.L. Katsev, *Image Transfer through a Scattering Medium* (Nauka i Tekhnika, Minsk, 1985), 327 pp.
4. L.S. Dolin, *Izv. Vyssh. Uchebn. Zaved., Radiofiz.* **9**, No. 1, 61–67 (1966).
5. W.G. Tam and A. Zardecki, *J. Opt. Soc. Am.* **69**, No. 1, 68–70 (1979).
6. V.F. Belov, A.G. Borovoi, N.I. Vagin, and S.N. Volkov, *Izv. Akad. Nauk SSSR, Fiz. Atmos. Okeana* **20**, No. 3, 323–327 (1984).
7. V.V. Veretennikov, *Opt. Atmos. Okeana* **6**, No. 4, 250–254 (1993).